^{18}F-FET PET imaging in differentiating glioma progression from treatment-related changes – a single-center experience

Gabriele D. Maurer[1,2,3], Daniel P. Brucker[2,3], Gabriele Stoffels[4], Katharina Filipski[3,5,6], Christian P. Filss[4,7], Felix M. Mottaghy[7,8,10], Norbert Galldiks[4,9,10,*], Joachim P. Steinbach[1,2,3,*], Elke Hattingen[11,*], and Karl-Josef Langen[4,7,10,*]

[1]Dr. Senckenberg Institute of Neurooncology, Goethe University Hospital, Frankfurt am Main, Germany

[2]University Cancer Center Frankfurt, Goethe University Hospital, Frankfurt am Main, Germany

[3]German Cancer Consortium (DKTK), Partner Site Frankfurt/Mainz, Heidelberg, Germany

[4]Institute of Neuroscience and Medicine INM-3, -4, Research Center Juelich, Juelich, Germany

[5]German Cancer Research Center (DKFZ), Heidelberg, Germany

[6]Institute of Neurology (Edinger Institute), Goethe University Hospital, Frankfurt am Main, Germany

[7]Department of Nuclear Medicine, RWTH University Hospital, Aachen, Germany

[8]Department of Radiology and Nuclear Medicine, MUMCx, Maastricht, The Netherlands

[9]Department of Neurology, University Hospital Cologne, Cologne, Germany

[10]Center of Integrated Oncology (CIO), Universities of Aachen, Bonn, Cologne, and Duesseldorf, Cologne, Germany

[11]Institute of Neuroradiology, Goethe University Hospital, Frankfurt am Main, Germany

[*]NG, JPS, EH and KJL contributed equally to this work.

For correspondence contact: Gabriele Maurer, Dr. Senckenberg Institute of Neurooncology, Goethe University Hospital, Schleusenweg 2-16, 60528 Frankfurt am Main, Germany, E-mail: gabriele.maurer@kgu.de

Authors' contributions: Conceptualization: GDM, JPS, EH and KJL, data analysis: GDM, DPB, GS, CPF, NG, FMM and KJL, neuropathological examinations: KF, supervision: NG, JPS and EH, writing – original draft, tables and figures: GDM and KJL, writing – review and editing: all.

Running title: ^{18}F-FET PET in recurrent glioma

ABSTRACT

In glioma patients, the differentiation between tumor progression (TP) and treatment-related changes (TRC) remains challenging. Difficulties in classifying imaging alterations may result in a delay or an unnecessary discontinuation of treatment. Positron emission tomography (PET) using O-(2-[^{18}F]fluoroethyl-)-L-tyrosine (^{18}F-FET) has been shown to be a useful tool for detecting TP and TRC.

Methods: We retrospectively evaluated 127 consecutive patients with WHO grade II-IV glioma who underwent ^{18}F-FET PET imaging in order to distinguish between TP and TRC. ^{18}F-FET PET findings were verified by neuropathology (40 patients) or clinico-radiological follow-up (87 patients). Maximum tumor to brain ratios (TBR_{max}) of ^{18}F-FET uptake and the slope of the time-activity curves (20-50 min post injection) were determined. Diagnostic accuracy of ^{18}F-FET PET parameters was evaluated by Receiver-Operating-Characteristic (ROC) analysis and chi-square test. The prognostic value of ^{18}F-FET PET was estimated using the Kaplan-Meier method.

Results: TP was diagnosed in 94 patients (74%) and TRC in 33 (26%). For differentiating TP and TRC, ROC analysis yielded an optimal ^{18}F-FET TBR_{max} cut-off value of 1.95 (sensitivity 70%, specificity 71%, accuracy 70%, AUC 0.75 ± 0.05). The highest accuracy was achieved by a combination of TBR_{max} and slope (sensitivity 86%, specificity 67%, accuracy 81%). However, accuracy was poorer when tumors harbored isocitrate dehydrogenase (*IDH*) mutations (91% in *IDH*-wildtype, 67% in *IDH*-mutant tumors, $p < 0.001$). ^{18}F-FET PET results correlated with overall survival ($p < 0.001$).

Conclusion: In our neuro-oncology department, diagnostic performance of ^{18}F-FET PET was convincing but slightly inferior to that of previous reports.

Keywords

^{18}F-FET PET, glioma, tumor progression, pseudoprogression, treatment-related changes

INTRODUCTION

Gliomas account for approximately 26% of primary central nervous system tumors and, among these, for 81% of malignant neoplasms (*1*). Clinical decision-making considerably depends on glioma classification, based on histological and molecular parameters (*2*), and imaging features. Despite some advances in surgical management and treatment regimens, grade II-IV gliomas remain incurable diseases with a decreased life expectancy.

The effectiveness of a treatment strategy is evaluated using the Response Assessment in Neuro-Oncology (RANO) criteria (*3–5*), which integrate magnetic resonance imaging (MRI) parameters, corticosteroid dosage, and the patient's performance status. Nevertheless, the differentiation between treatment-induced changes (TRC) and actual tumor progression (TP) continues to be a crucial issue(*6*). A frequent problem is the so-called pseudoprogression which describes the phenomenon that, in the absence of actual tumor growth, the diameter of contrast-enhancing areas enlarge more than 25% or new lesions occur during or after therapy, mimicking tumor progression within the first three months after chemoradiation completion with subsequent improvement of MRI findings (*7–9*). Within the spectrum of TRC, radionecrosis is also of clinical relevance. Radionecrosis denotes an injury of brain tissue that is related to irradiation and may occur several months or even years after radiotherapy completion (*10*,*11*).

As TRC may raise concerns about whether therapy should be initiated, continued, or changed, various imaging techniques including MRI methods and positron emission tomography (PET) are under consideration in order to better distinguish TRC from TP (*12–14*). In this context, PET using O-(2-[^{18}F]fluoroethyl-)-L-tyrosine (^{18}F-FET) has been shown to provide additional information (*15–18*) and has recently been recommended by the RANO group (*19*). Some studies already investigated the performance of ^{18}F-FET PET in glioma. However, they were either based on smaller patient populations (*16*,*17*,*20–25*) or included only a minor fraction of patients with TRC *(15)*.

In our neuro-oncology department, we recommended ^{18}F-FET PET imaging when conventional MRI and clinical assessment left some ambiguity as to whether TP or sequelae of therapy prevailed. We

here outline our experiences and focus on the diagnostic performance of additional ^{18}F-FET PET scans in clinical routine.

MATERIALS AND METHODS

Subjects

This retrospective study included 127 patients who were treated at the neuro-oncology department of the Goethe University Hospital in Frankfurt and, on the recommendation of the multidisciplinary tumor board and in order to distinguish between TP and TRC, were referred to the nuclear medicine department of the University Hospital in Aachen at the Forschungszentrum Jülich for ^{18}F-FET PET imaging between March 2016 and January 2019. The analysis was approved by the scientific board of the University Cancer Center Frankfurt and the local ethics committee, project number SNO-8-2018. All patients had undergone standard MRI before, were able to understand the reason for additional ^{18}F-FET PET imaging and gave written informed consent to the examination. 125 patients had previously been diagnosed with WHO grade II-IV glioma, two patients had been treated for suspected glioma without prior biopsy.

^{18}F-FET PET Imaging

The amino acid ^{18}F-FET was synthetized and applied as described previously (*26*). All patients underwent a dynamic PET scan from 0 to 50 min post injection of 3 MBq of ^{18}F-FET per kg of body weight. The interval between MRI and ^{18}F-FET PET investigation ranged from 0 to 77 days (median, 12 days). One-hundred-two patients were measured on a stand-alone PET scanner (ECAT EXACT HR+, Siemens Healthcare, Erlangen, Germany) in 3D mode and 25 patients on a high-resolution 3T hybrid PET/MR scanner (BrainPET, Siemens Healthcare); for further details, see (*22*,*25*). Due to the reconstruction parameters and post-processing steps, the different scanner types did not affect the quantitative ^{18}F-FET PET parameters (*27*).

Post-processing of ^{18}F-FET PET Images

Mean tumoral ^{18}F-FET uptake was determined by a two-dimensional auto-contouring process using a tumor-to-brain ratio (TBR) of at least 1.6 as described previously (*22*,*25*). For maximal amino acid uptake, a circular region of interest (ROI) with a diameter of 1.6 cm was centered on maximal tumor uptake (*15*), in order to exclude an influence of different scanner resolution. Mean and maximum TBR (TBR_{mean} and TBR_{max}) were calculated by dividing the mean and maximum standardized uptake value (SUV) of the tumor ROI by the mean SUV of a larger crescent shape volume of interest (VOI) placed in the semioval center of the contralateral unaffected hemisphere including white and grey matter (*28*,*29*).

Furthermore, time-activity curves (TAC) of ^{18}F-FET uptake in the tumor were obtained by the application of a spherical VOI with a diameter of 1.6 cm to the entire dynamic dataset. Derived from TAC, time-to-peak values (TTP; min from the beginning of the dynamic acquisition up to the maximum SUV of the lesion) and the slope of the TAC in the late phase of ^{18}F-FET uptake by fitting a linear regression line to the late phase of the curve (20-50 min post injection) were calculated. The slope was expressed in change of SUV per hour.

Diagnosis of Tumor Progression and Treatment-related Changes

TP or TRC were confirmed by histopathology, following resection or biopsy, or clinico-radiological follow-up. For WHO grade II gliomas, both the clinical and the radiological situation had to be stable/improved for at least 12 months without administration of another therapy in order to exclude TP (*16*). For WHO grade III-IV gliomas, the classification of TRC required at least six months of stable or improved clinical and radiological condition (*17*), as well as no change in tumor treatment. TP was considered present when lesions continued to increase in size on at least two subsequent MRI scans according to the RANO criteria, paralleled by a deterioration in performance status, or when a patient died of glioma, whichever occurred first. Thus, the classification criteria in our study were similar to (*25*,*30*,*31*) or more stringent (*20*) than those of previous investigations.

Neuropathology

Tissue obtained from resection or biopsy was fixed in 4% paraformaldehyde and paraffin embedded. Sections of 3 µm thickness were cut on a Leica SM 2000R microtome (Leica Biosystems, Wetzlar, Germany), mounted on microscope slides (SuperFrost Plus, Thermo Scientific, MA, USA) and subjected to hematoxylin-eosin (HE) staining. Immunohistochemistry against the isocitrate dehydrogenase (*IDH*) mutation-specific antibody IDH1_R132H (mouse monoclonal, clone DIA-H09, concentration 1:50, Dianova, Hamburg, Germany) was performed according to standardized protocols using a Leica BOND-III stainer. A tumor was considered to be progressive when solid tumor was seen in histological workup; the occurrence of single, e.g. IDH1_R132H positive tumor cells was not sufficient for diagnosis of TP. TRC, on the other hand, were characterized by missing solid tumor, radiogenic necrosis, hyalinized vessel walls and/or resorptive changes.

Statistical Analysis

Data analysis was carried out with Excel (Microsoft, Seattle, WA, USA), SPSS Statistics 25 (IBM, Armonk, NY, USA) and SigmaPlot Version 11.0 (Systat Software, San José, CA, USA). Continuously scaled variables were compared by the Mann-Whitney rank sum test or the Student's t-test for independent samples, categorical variables by the Pearson's chi-squared test or the Fisher's exact test. Survival was calculated from the date of ^{18}F-FET PET imaging to the date of death or the last follow-up visit, and survival distributions were analyzed using the log-rank test. Univariate and multivariate Cox regression models were applied to identify prognostic parameters. A p-value below 0.05 was considered significant. The diagnostic performance of the ^{18}F-FET PET parameters TBR_{max}, TBR_{mean}, TTP and slope for the differentiation of TP and TRC was assessed by Receiver-Operating-Characteristic (ROC) curve analyses using the neuropathological results or the clinico-radiological follow-up as reference. The decision cut-off was considered optimal when the product of paired values for sensitivity and specificity reached its maximum. Visualization was performed using Excel, Illustrator (Adobe, San José, CA, USA) and http://app.rawgraphs.io/ (*32*).

RESULTS

Patient and tumor characteristics are depicted in Figure 1, Table 1, and Supplemental Table 1.

Re-resection was performed in 36, biopsy in four patients. The median time from ^{18}F-FET PET scan to surgery was 21.5 days (range, 10-215) and longer when ^{18}F-FET PET indicated TRC (6 patients, median, 90 days, range, 12-215) than when ^{18}F-FET PET suggested TP (34 patients, median, 19 days, range, 10-119). Eighty-seven patients were evaluated on the basis of clinico-radiological follow-up. Until June 2019, 57 of the 127 patients succumbed to their disease (median time from ^{18}F-FET PET scan to death, 208 days, range, 24-950 days), and 70 continued follow-up (median time from ^{18}F-FET PET scan to last follow-up visit, 484 days, range, 128-1050 days).

ROC analysis yielded a TBR_{max} of 1.95 as an optimal cut-off to identify TP (sensitivity 70%, specificity 71%, AUC 0.76 ± 0.05, $p < 0.001$). The cut-off for the TBR_{mean} to detect TP was also 1.95 (sensitivity 56%, specificity 79%, accuracy 62%, AUC 0.75 ± 0.05, $p < 0.001$). TTP did not allow to discriminate between TP and TRC (AUC 0.58, $p = 0.15$). For slope, the optimal cut-off to show TP was < 0.2 SUV/h (sensitivity 54%, specificity 86%, accuracy 63%, AUC 0.69 ± 0.05, $p < 0.001$). The combined analysis of $TBR_{max} > 1.95$ and/or slope < 0.2 SUV/h revealed TP best with a sensitivity of 86%, a specificity of 67% and an accuracy of 81% ($p < 0.001$). In individual cases (6 patients), further criteria such as a focal hotspot which was underestimated by the ROI analysis, or an increasing ^{18}F-FET uptake compared to a previous ^{18}F-FET PET examination, were also considered as indicators of TP (see Supplemental Table 1). Supplemental Tables 2 and 3 summarize the diagnoses based on ^{18}F-FET PET findings. Figure 2 depicts examples of false positive and negative ^{18}F-FET PET ratings.

Overall survival was longer when finally TRC were diagnosed (Figure 3A), as well as when ^{18}F-FET PET results indicated TRC (Figure 3B). Results of univariate and multivariate survival analyses are given in Table 2. In multivariate evaluation, we fitted a stepwise backward exclusion model including the ^{18}F-FET PET rating, the tumor grade, the *IDH* status, the O6-methylguanine-DNA methyltransferase (*MGMT*) promoter methylation status, the patient's age and Karnofsky performance status. The ^{18}F-FET PET rating, the WHO grade, the *IDH* status and the Karnofsky performance status remained independent prognostic factors.

Looking at the tumor characteristics, we noticed that the accuracy of ^{18}F-FET PET was higher in *IDH*-wildtype gliomas than in *IDH*-mutant ones ($p < 0.001$). The diagnosis based on ^{18}F-FET PET turned out to be incorrect in 33% of the *IDH*-mutant tumors (11 true negative, 23 true positive, 8 false positive and 9 false negative ^{18}F-FET PET results), but only in 9% of the *IDH*-wildtype tumors (8 true negative, 56 true positive, 3 false positive and 3 false negative ^{18}F-FET PET results). *MGMT* promoter methylation did not significantly affect the diagnostic performance of ^{18}F-FET PET.

DISCUSSION

Diagnosis and treatment of brain tumors are strongly linked to imaging, especially MRI, techniques, as histological confirmation often cannot be realized easily and without substantial risk. ^{18}F-FET PET is not a standard method for the assessment of TP in glioma, but may be more accurate than conventional MRI (*14*,*25*) and helpful in complex or challenging cases (*19*). In our department, we consider this method in particular when MRI yields inconclusive results. The present report outlines our experience with ^{18}F-FET PET in differentiating TP and TRC in WHO grade II-IV gliomas. ^{18}F-FET PET based on TBR_{max} achieved an accuracy of 70% which could be increased to 81% by a combination with kinetic parameters. However, these values are in the lower range compared with previous studies.

Retrospectively analyzing 132 scans of 124 WHO grade II-IV glioma patients, Galldiks *et al.* described an accuracy of ^{18}F-FET PET to diagnose TP of 93% (*15*) but the number of patients with TRC in that study, namely 8%, was quite small and might have influenced the results. Looking at 45 patients suspected of having TP, Rachinger *et al.* found a sensitivity of 100% and a specificity of 93% for ^{18}F-FET PET imaging (*21*). Kebir *et al.* noted a sensitivity of 84%, a specificity of 86% and an accuracy of 85% for ^{18}F-FET PET to differentiate between TP and pseudoprogression in a series of 26 patients (*20*). In a study on 36 glioblastoma patients conducted by Mihovilovic *et al.*, static ^{18}F-FET PET discriminated between TP and TRC with a sensitivity of 89%, a specificity of 75% and an accuracy of 86% (*31*). Analyzing ^{18}F-FET PET scans of 48 high-grade glioma patients, Werner *et al.* reported a prevalence of TRC of 21% and a 93% diagnostic accuracy of static and dynamic ^{18}F-FET PET parameters (*25*). In our

study, the percentage of patients with TRC was similar to that in other studies (*20*,*25*,*31*), but the diagnostic performance of ^{18}F-FET PET imaging was slightly inferior (*20*,*23*,*31*).

It has to be considered that all patients in this study were treated in a single neuro-oncology department with procedures that based on weekly discussions in multidisciplinary tumor conferences. Therefore, the decision-making process should have been consistent but carried several biases. First, ^{18}F-FET PET imaging was not part of the routine workup of patients with suspected TP. Many patients initially underwent MR perfusion and spectroscopy and often ^{18}F-FET PET was recommended merely in cases of ambiguity. Therefore, the patient group might represent a selection of particularly difficult cases, which in turn could lead to an underestimation of the accuracy of ^{18}F-FET PET. Second, imaging was considered appropriate only if it resulted in therapeutic consequences. That's why patients with a poor performance status and/or without further treatment options were not assigned to receive ^{18}F-FET PET imaging. Third, a higher rate of histological confirmation following ^{18}F-FET PET would have been desirable, but resection or biopsy was not routinely performed when the imaging aspect was ambiguous. Invasive interventions were only suggested if all evidence pointed towards TP. However, the sole inclusion of patients with histological confirmation would lead to a different bias, especially to the exclusion of true negative results. Despite these limitations, this study probably reflects the current situation in many centers, as ^{18}F-FET PET is not generally available as a routine tool and can only be used in selected indications.

An interesting new observation in our study was the fact that the accuracy of ^{18}F-FET PET in differentiating TP and TRC was significantly higher in *IDH*-wildtype tumors than in *IDH*-mutant ones. This knowledge could be helpful when considering ^{18}F-FET PET as an additional diagnostic tool. Possibly, previous studies did not reveal this aspect due to a lack of molecular markers, smaller collectives or a minor fraction of patients with TRC. It is certainly worth further investigation and should be verified in a larger number of patients. In view of the current literature, we cannot clearly explain this finding, especially false positive ^{18}F-FET PET results. Compared with *IDH*-wildtype tumors, *IDH*-mutant gliomas are considered less immunologically active (*33*), and the presence of mutant *IDH* has been shown to impair complement activation, infiltration of CD45+ immune cells, T-cell migration,

proliferation and activity (*34*). As inflammation may contribute to the ^{18}F-FET PET signal under certain circumstances (*14*), immunosuppression might mask tumor growth and lead to false negative results.

CONCLUSION

^{18}F-FET-PET complemented our current diagnostic portfolio, drove decision-making and independently predicted survival. The interpretation of results should consider the tumor's *IDH* status as, in our study, the accuracy of ^{18}F-FET PET was higher in *IDH*-wildtype gliomas.

ACKNOWLEDGEMENTS

We thank all the patients and their families for participating in this study, the nurses and assistants at the Dr. Senckenberg Institute of Neurooncology for supporting the outpatient procedures, Erika Wabbals, Silke Grafmueller and Sascha Rehbein for technical assistance in radiosynthesis of ^{18}F-FET and Silke Frensch, Suzanne Schaden, Kornelia Frey and Trude Plum for technical assistance in performing the PET measurements at the Forschungszentrum Jülich.

DISCLOSURE

The Dr. Senckenberg Institute of Neurooncology is supported by the Dr. Senckenberg foundation (grant number 2014/SIN-02). JPS has received a grant from Merck as well as honoraria for lectures, travel or advisory board participation from Roche, Medac, Bristol-Myers Squibb and Abbvie. No other potential conflicts of interest relevant to this article exist.

KEY POINTS

Question: How well can ^{18}F-FET PET help to distinguish between glioma progression and treatment-related changes?

Findings: In this retrospective analysis of patients with WHO grade II-IV glioma, treated at our neuro-oncology department, the diagnostic accuracy of ^{18}F-FET PET was slightly inferior to that of previous reports and higher in *IDH*-wildtype than in *IDH*-mutant tumors. The ^{18}F-FET PET rating was prognostic of survival.

Implications for patient care: ^{18}F-FET PET provided valuable information. Our observation that its accuracy depended on the *IDH* status might be crucial for decision-making.

REFERENCES

1. Ostrom QT, Gittleman H, Truitt G, Boscia A, Kruchko C, Barnholtz-Sloan JS. CBTRUS statistical report: Primary brain and other central nervous system tumors diagnosed in the United States in 2011–2015. *Neuro-Oncol*. 2018;20:iv1-iv86.

2. Louis DN, Perry A, Reifenberger G, et al. The 2016 World Health Organization classification of tumors of the central nervous system: a summary. *Acta Neuropathol*. 2016;131:803-820.

3. Wen PY, Macdonald DR, Reardon DA, et al. Updated response assessment criteria for high-grade gliomas: response assessment in neuro-oncology working group. *J Clin Oncol*. 2010;28:1963-1972.

4. van den Bent M, Wefel J, Schiff D, et al. Response assessment in neuro-oncology (a report of the RANO group): assessment of outcome in trials of diffuse low-grade gliomas. *Lancet Oncol*. 2011;12:583-593.

5. Ellingson BM, Wen PY, Cloughesy TF. Modified criteria for radiographic response assessment in glioblastoma clinical trials. *Neurotherapeutics*. 2017;14:307-320.

6. Hygino da Cruz LC, Rodriguez I, Domingues RC, Gasparetto EL, Sorensen AG. Pseudoprogression and pseudoresponse: imaging challenges in the assessment of posttreatment glioma. *AJNR Am J Neuroradiol*. 2011;32:1978-1985.

7. Thust SC, van den Bent MJ, Smits M. Pseudoprogression of brain tumors. *J Magn Reson Imaging*. 2018;48:571-589.

8. Brandsma D, Stalpers L, Taal W, Sminia P, van den Bent MJ. Clinical features, mechanisms, and management of pseudoprogression in malignant gliomas. *Lancet Oncol*. 2008;9:453-461.

9. Hoffman WF, Levin VA, Wilson CB. Evaluation of malignant glioma patients during the postirradiation period. *J Neurosurg*. 1979;50:624-628.

10. Siu A, Wind JJ, Iorgulescu JB, Chan TA, Yamada Y, Sherman JH. Radiation necrosis following treatment of high grade glioma--a review of the literature and current understanding. *Acta Neurochir (Wien)*. 2012;154:191-201.

11. Delgado-López PD, Riñones-Mena E, Corrales-García EM. Treatment-related changes in glioblastoma: a review on the controversies in response assessment criteria and the concepts of true progression, pseudoprogression, pseudoresponse and radionecrosis. *Clin Transl Oncol*. 2018;20:939-953.

12. van Dijken BRJ, van Laar PJ, Holtman GA, van der Hoorn A. Diagnostic accuracy of magnetic resonance imaging techniques for treatment response evaluation in patients with high-grade glioma, a systematic review and meta-analysis. *Eur Radiol*. 2017;27:4129-4144.

13. Prager AJ, Martinez N, Beal K, Omuro A, Zhang Z, Young RJ. Diffusion and perfusion MRI to differentiate treatment-related changes including pseudoprogression from recurrent tumors in high-grade gliomas with histopathologic evidence. *AJNR Am J Neuroradiol*. 2015;36:877-885.

14. Langen K-J, Galldiks N, Hattingen E, Shah NJ. Advances in neuro-oncology imaging. *Nat Rev Neurol*. 2017;13:279-289.

15. Galldiks N, Stoffels G, Filss C, et al. The use of dynamic O-(2-18F-fluoroethyl)-l-tyrosine PET in the diagnosis of patients with progressive and recurrent glioma. *Neuro Oncol*. 2015;17:1293-1300.

16. Pöpperl G, Götz C, Rachinger W, Gildehaus F-J, Tonn J-C, Tatsch K. Value of O-(2-[18F]fluoroethyl)- L-tyrosine PET for the diagnosis of recurrent glioma. *Eur J Nucl Med Mol Imaging*. 2004;31:1464-1470.

17. Mehrkens JH, Pöpperl G, Rachinger W, et al. The positive predictive value of O-(2-[18F]fluoroethyl)-L-tyrosine (FET) PET in the diagnosis of a glioma recurrence after multimodal treatment. *J Neurooncol*. 2008;88:27-35.

18. la Fougère C, Suchorska B, Bartenstein P, Kreth F-W, Tonn J-C. Molecular imaging of gliomas with PET: opportunities and limitations. *Neuro Oncol*. 2011;13:806-819.

19. Albert NL, Weller M, Suchorska B, et al. Response Assessment in Neuro-Oncology working group and European Association for Neuro-Oncology recommendations for the clinical use of PET imaging in gliomas. *Neuro Oncol*. 2016;18:1199-1208.

20. Kebir S, Fimmers R, Galldiks N, et al. Late pseudoprogression in glioblastoma: diagnostic value of dynamic O-(2-[18F]fluoroethyl)-L-tyrosine PET. *Clin Cancer Res*. 2016;22:2190-2196.

21. Rachinger W, Goetz C, Pöpperl G, et al. Positron emission tomography with O-(2-[18F]fluoroethyl)-L-tyrosine versus magnetic resonance imaging in the diagnosis of recurrent gliomas. *Neurosurgery*. 2005;57:505-511.

22. Ceccon G, Lazaridis L, Stoffels G, et al. Use of FET PET in glioblastoma patients undergoing neurooncological treatment including tumour-treating fields: initial experience. *Eur J Nucl Med Mol Imaging*. 2018;45:1626-1635.

23. Pyka T, Hiob D, Preibisch C, et al. Diagnosis of glioma recurrence using multiparametric dynamic 18F-fluoroethyl-tyrosine PET-MRI. *Eur J Radiol*. 2018;103:32-37.

24. Jena A, Taneja S, Gambhir A, et al. Glioma recurrence versus radiation necrosis: single-session multiparametric approach using simultaneous O-(2-18F-fluoroethyl)-L-tyrosine PET/MRI. *Clin Nucl Med*. 2016;41:e228-236.

25. Werner J-M, Stoffels G, Lichtenstein T, et al. Differentiation of treatment-related changes from tumour progression: a direct comparison between dynamic FET PET and ADC values obtained from DWI MRI. *Eur J Nucl Med Mol Imaging*. 2019;46:1889-1901.

26. Hamacher K, Coenen HH. Efficient routine production of the 18F-labelled amino acid O-2-18F fluoroethyl-L-tyrosine. *Appl Radiat Isot*. 2002;57:853-856.

27. Lohmann P, Herzog H, Rota Kops E, et al. Dual-time-point O-(2-[(18)F]fluoroethyl)-L-tyrosine PET for grading of cerebral gliomas. *Eur Radiol*. 2015;25:3017-3024.

28. Unterrainer M, Vettermann F, Brendel M, et al. Towards standardization of 18F-FET PET imaging: do we need a consistent method of background activity assessment? *EJNMMI Res*. 2017;7:48.

29. Law I, Albert NL, Arbizu J, et al. Joint EANM/EANO/RANO practice guidelines/SNMMI procedure standards for imaging of gliomas using PET with radiolabelled amino acids and [18F]FDG: version 1.0. *Eur J Nucl Med Mol Imaging*. 2019;46:540-557.

30. Young RJ, Gupta A, Shah AD, et al. Potential utility of conventional MRI signs in diagnosing pseudoprogression in glioblastoma. *Neurology*. 2011;76:1918-1924.

31. Mihovilovic MI, Kertels O, Hänscheid H, et al. O-(2-(18F)fluoroethyl)-L-tyrosine PET for the differentiation of tumour recurrence from late pseudoprogression in glioblastoma. *J Neurol Neurosurg Psychiatry*. 2019;90:238-239.

32. Mauri M, Elli T, Caviglia G, Uboldi G, Azzi M. RAWGraphs: a visualisation platform to create open outputs. In: Proceedings of the 12th biannual conference on Italian SIGCHI chapter - CHItaly '17. Cagliari, Italy: ACM Press; 2017:1-5.

33. Kaminska B, Czapski B, Guzik R, Król S, Gielniewski B. Consequences of IDH1/2 mutations in gliomas and an assessment of inhibitors targeting mutated IDH proteins. *Molecules*. 2019;24:968.

34. Lucca LE, Hafler DA. Resisting fatal attraction: a glioma oncometabolite prevents CD8+ T cell recruitment. *J Clin Invest*. 2017;127:1218-1220.

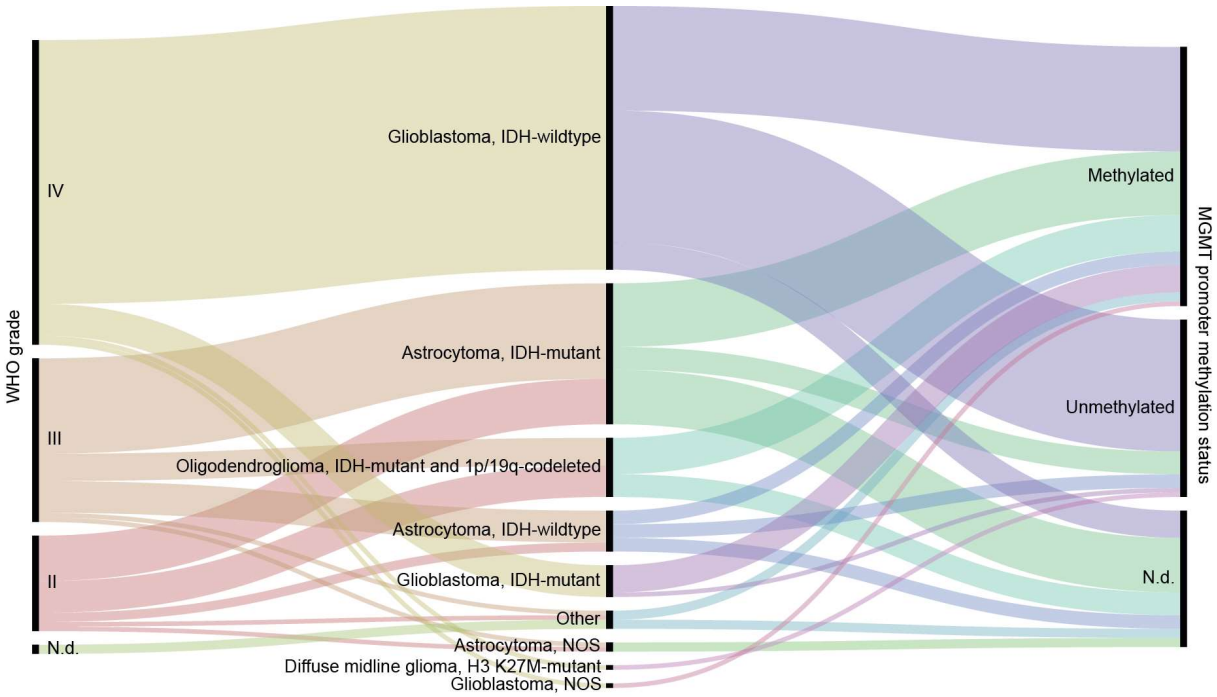

Figure 1: WHO grade, diagnosis according to the WHO 2016 classification of brain tumors (*2*) and *MGMT* promoter methylation status of the tumors that were later examined with ^{18}F-FET PET; n.d., not determined or inconclusive.

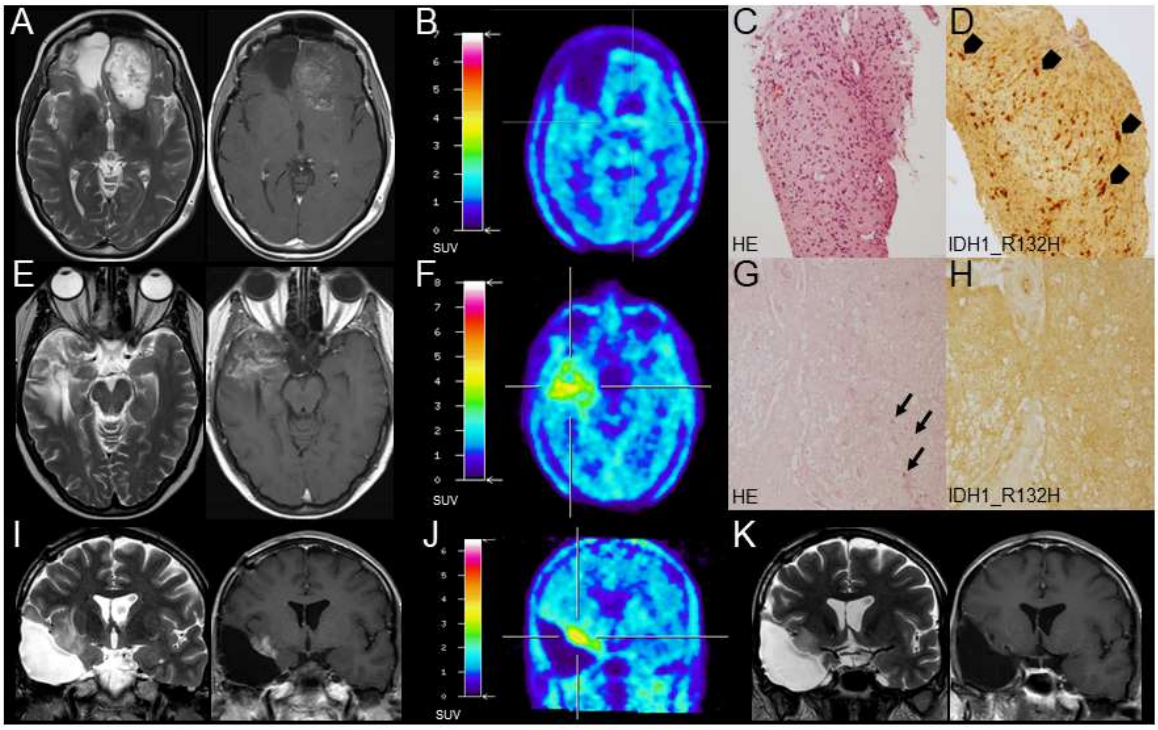

Figure 2: Examples of false negative and positive ^{18}F-FET PET ratings. (**A-D**) A 45-year-old-patient had been diagnosed with an *IDH*-mutant, *MGMT* promoter methylated glioblastoma in November 2010. After gross total resection, radiotherapy and irinotecan chemotherapy, she received bevacizumab every other week. In January 2017, a follow-up MRI scan indicated disease progression (RANO criteria). However, in February 2017, ^{18}F-FET PET imaging was not suggestive of tumor, and so the patient continued follow-up. Subsequent MRI revealed an enlargement of both contrast-enhancing and nonenhancing lesions (tumor progression, RANO criteria), but ^{18}F-FET PET remained negative. In November 2017, biopsy revealed tumor progression. (**A**) Axial MRI, October 2017, T2 (left) and contrast-enhanced T1 (right), (**B**) ^{18}F-FET PET, November 2017, (**C**) histology (HE), (**D**) immunohistochemistry (IDH1_R132H, arrowheads point to IDH1_R132H positive tumor cells), biopsy, November 2017. (**E-H**) A 39-year-old patient had undergone subtotal resection of an IDH1_R132H-mutant and 1p/19q-codeleted oligodendroglioma in August 2010, temozolomide chemotherapy until January 2011, proton therapy in May and June 2015 and lomustine chemotherapy from July to December 2015. In July 2017, putative recurrent tumor was resected. Neuropathology showed sequelae of radiation but no tumor. (**E**) Axial MRI, May 2017, T2 (left) and contrast-enhanced T1 (right), (**F**) ^{18}F-FET PET

indicating tumor progression, June 2017, (**G**) necrosis and calcification (arrows, HE) without (**H**) IDH1_R132H-positive tumor cells, resection, July 2017. (**I-K**) The *IDH*-mutant, *MGMT* promoter methylated glioblastoma of a 38-year-old patient had been treated by partial resection in April 2016, radiotherapy and temozolomide chemotherapy from April to June 2016. Against our advice, the patient decided not to continue tumor-specific therapy. However, imaging alterations regressed spontaneously. (**I**) Coronar MRI, February 2017, T2 (left) and contrast-enhanced T1 (right), (**J**) ^{18}F-FET PET indicating tumor progression, April 2017, (**K**) follow-up MRI, February 2018, T2 (left) and contrast-enhanced T1 (right).

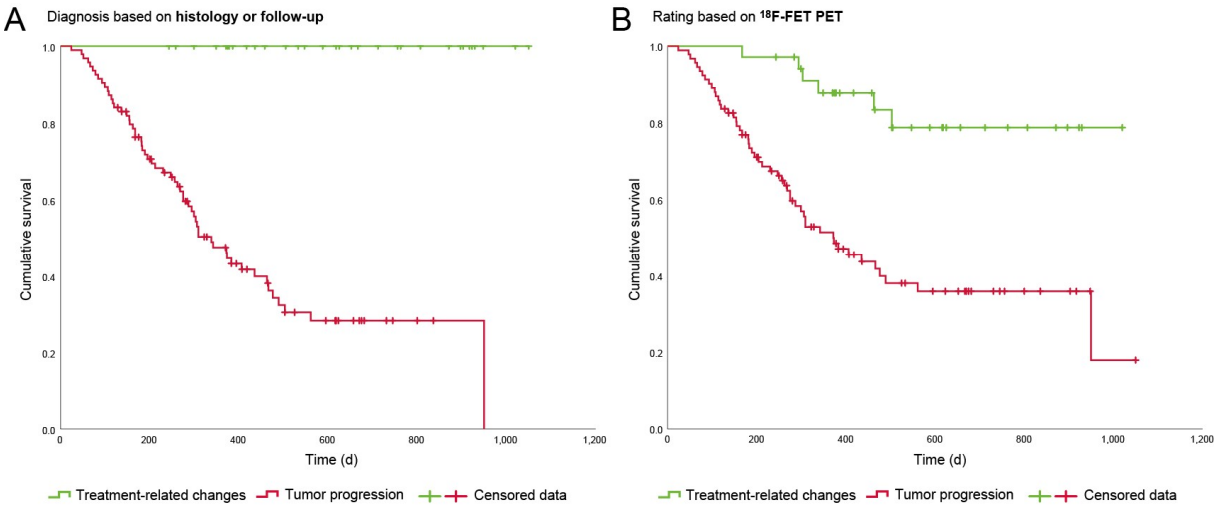

Figure 3: Overall survival of all 127 patients. (**A**) Overall survival after ^{18}F-FET PET imaging, depending on whether TP or TRC were present, as assessed by histology or follow-up, p (log-rank) < 0.001. (**B**) Overall survival after ^{18}F-FET PET imaging, depending on ^{18}F-FET PET results, p (log-rank) < 0.001.

TABLE 1
Patient and tumor characteristics

			number	%
Sex	male		83	65
	female		44	35
Age when ^{18}F-FET PET imaging was performed (mean + SD, range)			50 + 12, 20 - 78	
KPS when ^{18}F-FET PET imaging was performed		%		
		100	49	39
		90	46	36
		80	19	15
		70	11	9
		60	2	2
Diagnosis		WHO grade		
	glioblastoma, *IDH*-wildtype	IV	59	46
	glioblastoma, *IDH*-mutant	IV	7	6
	glioblastoma, NOS	IV	1	0.8
	astrocytoma, *IDH*-wildtype	II	2	2
		III	7	6
	astrocytoma, *IDH*-mutant	II	10	8
		III	21	17
	astrocytoma, NOS	II	1	0.8
		III	1	0.8
	oligodendroglioma, *IDH*-mutant and 1p/19q-codeleted	II	7	6
		III	6	5
	diffuse midline glioma, H3 K27M-mutant	IV	1	0.8
	other*	II	1	0.8
		III	1	0.8
		n.d.	2	2
***MGMT* promoter methylation status**				
	methylated		57	45
	unmethylated		40	31
	n.d.		30	24
Extent of resection at initial diagnosis				
	gross total resection		67	53
	subtotal resection		8	6
	partial resection		20	16
	biopsy		30	24
	none		2	2
Interval between last therapy and ^{18}F-FET PET scan (days, median, range)			103, 0 - 3540	
Therapy prior to ^{18}F-FET PET imaging				
	radiotherapy		114	90
	chemotherapy	temozolomide	106	83
		lomustine-containing regimen	29	23
	bevacizumab		9	7
	tumor treating fields		9	7
	re-resection		21	17
	re-irradiation		19	15
	nivolumab		7	6
	other†		6	5

KPS, Karnofsky performance status, n.d., not determined or inconclusive. *This section included one diffuse glioma, *IDH*-wildtype, nuclear ATRX retained, *MGMT* promoter methylated, one anaplastic glioma, *IDH*-mutant, nuclear ATRX retained, *MGMT* promoter methylated, one suspected diffuse pontine glioma (treated without prior biopsy) and one suspected diffuse medulla oblongata glioma (treated without prior biopsy). †This section included three patients treated with nivolumab or placebo in the context of a clinical trial, one patient treated with Cerepro^{R}/ganciclovir, one patient treated with brachytherapy employing iodine-125 seeds and one patient treated with irinotecan.

TABLE 2

Univariate and multivariate analyses of overall survival

Univariate survival analysis	***number of patients***	***HR***	***95% CI***	***p***
Diagnosis based on ^{18}F-FET PET	127	4.997	2.139 – 11.675	< 0.001
***IDH* status**				
IDH-wildtype	70	1.000		
IDH-mutant	51	0.181	0.091 – 0.363	< 0.001
***MGMT* promoter methylation status**				
unmethylated	40	1.000		
methylated	57	0.493	0.278 – 0.877	0.016
WHO grade	125	3.859	2.230 – 6.678	< 0.001
Age [years]	127	1.043	1.020 – 1.066	< 0.001
KPS [%]	127	0.965	0.940 – 0.990	0.007
Number of glioma recurrences prior to ^{18}F-FET PET scan	127	1.051	0.792 – 1.395	n.s.
Interval between last therapy and ^{18}F-FET PET scan [days]	124	0.997	0.996 – 0.999	0.001
Multivariate survival analysis				
Diagnosis based on ^{18}F-FET PET		3.424	1.446 – 8.109	0.005
WHO grade		2.143	1.212 – 3.792	0.009
***IDH* status**		0.412	0.210 – 0.808	0.010
KPS [%]		0.975	0.950 – 1.001	0.057

KPS, Karnofsky performance status; HR, hazard ratio; CI, confidence interval.

							Therapy prior to ^{18}F-FET PET											^{18}F-FET-PET evaluation				
Patient number	Sex	Age [years]	Diagnosis	WHO grade	MGMT promoter methylation status	IDH status	Radiotherapy	Temozolomide	Lomustine-containing regimen	Bevacizumab	Tumor treating fields	Re-resection	Re-irradiation	Nivolumab	Number of recurrences before FET PET	Karnofsky performance status [%]	Final diagnosis	Final diagnosis established by	TBR_{mean}	TBR_{max}	Slope (SUV/h)	Special findings leading to positive PET rating	^{18}F-FET PET rating
1	m	51	GBM	IV	neg	wt	yes	yes	no	no	no	no	no	no	0	90	TP	NP	2,1	2,6	-0,72		TP
2	m	35	A	III	n.d.	mut	yes	no	yes	no	no	no	no	no	0	100	TRC	NP	1,6	1,6	0,75		TRC
3	m	38	GBM	IV	pos	wt	yes	yes	yes	no	no	no	no	no	1	100	TP	FU	2,2	2,9	0,66		TP
4	f	57	other	III	pos	mut	yes	yes	no	no	no	no	no	no	0	90	TRC	NP	2,1	2,7	-1,44		TP
5	f	47	A, NOS	II	n.d.	n.d.	yes	no	no	no	no	no	no	no	0	100	TRC	FU	1,7	1,7	0,92		TRC
6	m	51	A	III	neg	wt	yes	yes	no	no	no	yes	no	no	2	70	TP	FU	2,0	2,3	0,19		TP
7	m	39	A	III	neg	mut	yes	no	yes	no	no	no	no	no	0	90	TRC	FU	1,6	1,6	1,12		TRC
8	f	32	GBM	IV	neg	mut	yes	yes	no	yes	no	no	no	no	1	80	TP	NP	1,4	1,4	0,75		TRC
9	m	45	GBM	IV	pos	wt	yes	yes	no	no	no	no	no	no	0	100	TP	NP	2,5	3,3	0,45		TP
10	m	57	GBM	IV	pos	wt	yes	yes	no	no	no	no	no	no	0	100	TP	NP	1,6	1,6	0,15		TP
11	f	39	A	II	n.d.	mut	no	no	no	no	no	no	no	no	0	90	TRC	FU	1,0	1,0	0,20		TRC
12	m	33	A	II	n.d.	mut	yes	no	no	no	no	no	no	no	0	100	TRC	FU	1,2	1,2	0,40		TRC
13	f	39	A	III	n.d.	mut	yes	yes	no	no	no	yes	no	no	1	90	TP	FU	2,5	4,0	2,04		TP
14	m	34	A	III	pos	wt	no	no	no	no	no	no	no	no	0	80	TRC	FU	1,6	1,6	0,53		TRC
15	m	62	GBM	IV	neg	wt	yes	yes	no	no	no	no	no	no	0	100	TP	NP	2,0	2,3	-0,07		TP
16	f	30	A	III	n.d.	mut	yes	yes	no	no	no	no	no	no	0	100	TRC	FU	1,3	1,3	-0,07		TRC
17	m	60	GBM	IV	pos	wt	yes	yes	no	no	no	no	yes	no	1	80	TRC	FU	1,9	2,2	0,30		TP
18	m	24	DMG	IV	neg	wt	yes	yes	no	no	yes	no	no	no	0	80	TP	FU	2,1	2,1	0,56		TP
19	f	54	A	II	pos	mut	no	yes	yes	no	no	no	no	no	2	100	TP	NP	2,3	2,5	0,42		TP
20	m	53	GBM	IV	neg	wt	yes	yes	no	no	yes	no	no	no	0	100	TP	NP	2,0	2,3	0,82		TP
21	m	69	GBM	IV	pos	wt	yes	yes	yes	no	no	no	no	no	0	90	TP	FU	2,3	2,8	-0,04		TP
22	m	74	GBM	IV	pos	wt	yes	yes	no	no	no	no	no	no	0	90	TP	FU	2,0	2,1	0,09		TP
23	f	70	GBM	IV	pos	wt	yes	yes	no	no	no	no	no	no	0	90	TP	FU	1,9	2,2	0,06		TP
24	f	51	ODG	II	n.d.	n.d.	yes	yes	yes	no	no	no	yes	no	2	70	TRC	FU	1,9	1,9	0,99		TRC
25	m	38	GBM	IV	pos	wt	yes	yes	no	no	no	no	no	no	0	90	TP	FU	1,6	1,6	0,30		TRC
26	m	31	ODG	III	pos	mut	yes	yes	yes	no	no	yes	yes	no	3	80	TP	NP	1,9	1,9	0,13		TP
27	m	56	GBM	IV	neg	wt	yes	yes	yes	no	no	yes	yes	no	2	90	TP	FU	1,9	1,9	0,34		TP
28	m	78	other	II	pos	wt	no	yes	yes	no	no	no	no	no	1	100	TP	FU	1,8	1,8	-0,22		TP
29	m	47	GBM	IV	pos	mut	yes	yes	yes	no	no	no	no	no	2	90	TP	NP	1,9	2,4	1,20		TP
30	f	49	GBM	IV	pos	wt	yes	yes	yes	no	no	yes	no	no	0	70	TP	FU	2,1	2,2	-0,26		TP
31	m	52	GBM	IV	pos	wt	yes	yes	no	no	no	no	no	no	0	80	TP	NP	2,4	3,6	-2,66		TP
32	m	45	GBM	IV	neg	wt	yes	yes	no	no	no	no	no	no	0	90	TP	NP	2,3	2,6	-0,28		TP
33	f	65	GBM, NOS	IV	pos	n.d.	yes	yes	no	no	no	no	no	no	0	80	TP	FU	2,2	2,7	-0,29		TP
34	m	43	GBM	IV	neg	wt	yes	no	no	no	no	no	no	yes	0	100	TRC	FU	1,8	1,9	0,29		TRC
35	m	55	GBM	IV	pos	wt	yes	yes	yes	yes	no	no	yes	no	2	80	TP	FU	1,3	1,3	-0,30		TP
36	f	28	A	II	pos	mut	no	yes	no	no	no	no	no	no	0	90	TP	NP	2,9	3,6	-0,14		TP
37	m	52	GBM	IV	pos	wt	yes	yes	yes	no	no	no	no	no	0	90	TP	FU	2,4	3,1	-0,52		TP
38	f	48	GBM	IV	neg	wt	yes	yes	yes	yes	no	no	no	no	0	80	TRC	FU	1,9	1,9	1,20		TRC
39	m	45	other	n.d.	n.d.	n.d.	yes	yes	no	no	no	no	no	no	0	100	TP	FU	1,6	1,6	0,44	Hot spot	TP
40	m	39	GBM	IV	n.d.	wt	yes	yes	no	no	no	no	no	no	0	100	TP	FU	1,8	1,8	-0,28		TP
41	m	32	A, NOS	III	n.d.	n.d.	yes	yes	no	no	no	no	no	no	0	100	TP	FU	1,3	1,3	0,50		TRC
42	f	53	A	III	n.d.	mut	yes	yes	no	no	no	yes	yes	no	4	80	TP	FU	1,9	2,1	0,63		TP
43	m	65	A	III	pos	wt	yes	yes	no	no	no	no	no	no	0	90	TP	FU	1,5	1,5	-0,86		TP
44	m	51	GBM	IV	neg	wt	yes	yes	no	no	no	no	no	no	0	100	TP	FU	2,3	3,0	-0,36		TP
45	f	44	ODG	II	n.d.	mut	yes	yes	no	no	no	no	no	no	2	70	TP	FU	2,8	3,3	0,93		TP
46	f	63	GBM	IV	pos	wt	yes	yes	no	no	no	no	no	no	0	90	TP	NP	2,4	2,4	0,23		TP
47	m	51	A	III	n.d.	mut	yes	yes	no	no	no	no	no	no	1	90	TP	FU	2,1	2,2	-0,89		TP
48	m	41	A	II	n.d.	mut	no	no	no	no	no	no	no	no	0	90	TP	FU	1,3	1,3	0,69		TRC
49	m	68	GBM	IV	pos	wt	yes	yes	no	no	no	no	yes	no	1	90	TP	NP	2,0	2,7	0,49		TP
50	m	39	GBM	IV	neg	wt	yes	yes	no	no	no	no	no	no	0	100	TP	FU	1,4	1,4	-0,59		TRC
51	m	77	GBM	IV	pos	wt	yes	yes	no	no	no	no	no	no	0	60	TP	FU	2,5	3,1	0,63		TP
52	m	36	A	II	pos	mut	yes	yes	no	no	no	no	no	no	1	80	TP	NP	2,4	2,8	1,30		TP
53	f	45	GBM	IV	neg	wt	yes	yes	no	no	no	yes	no	no	0	60	TP	FU	2,0	2,2	2,19		TP
54	m	59	GBM	IV	neg	wt	yes	yes	no	no	no	no	no	no	0	80	TP	FU	2,0	2,3	-0,44		TP
55	m	54	GBM	IV	pos	wt	yes	yes	yes	no	no	no	yes	no	4	90	TP	NP	2,1	2,2	0,60		TP
56	m	44	GBM	IV	pos	wt	yes	yes	yes	no	no	no	no	no	0	100	TP	NP	2,3	2,7	-0,16		TP
57	f	53	A	II	pos	mut	no	yes	no	no	no	no	no	no	0	100	TP	FU	1,8	1,8	0,73	Hot spot	TP
58	m	54	GBM	IV	neg	wt	yes	yes	no	no	no	no	no	no	0	80	TP	FU	1,6	1,6	-0,94		TP
59	m	54	A	III	neg	wt	yes	yes	no	no	no	no	no	no	0	80	TRC	FU	2,0	2,1	1,15		TP
60	m	30	A	III	pos	mut	yes	yes	no	no	no	no	no	no	0	80	TRC	FU	2,1	2,5	0,78		TP
61	m	49	A	II	pos	mut	no	yes	yes	no	no	yes	no	no	2	70	TP	FU	2,4	3,0	-0,07		TP
62	m	66	ODG	III	pos	mut	yes	yes	no	no	no	no	yes	no	2	90	TP	FU	2,4	3,7	-0,92		TP
63	f	39	A	III	pos	mut	yes	yes	no	no	no	no	no	no	0	100	TRC	FU	2,4	1,9	1,63		TP
64	m	43	A	III	neg	mut	no	yes	no	no	no	no	no	no	0	100	TRC	FU	0,6	0,6	0,66		TRC
65	f	69	ODG	III	n.d.	mut	yes	no	yes	no	no	no	no	no	0	90	TRC	NP	1,4	1,4	0,88	Hot spot	TP
66	f	49	A	III	pos	mut	yes	yes	no	no	no	no	no	no	2	90	TP	NP	1,9	2,4	1,20		TP
67	m	49	GBM	IV	neg	wt	yes	yes	no	no	yes	no	no	no	0	90	TP	FU	2,0	2,0	-0,02		TP
68	f	59	GBM	IV	neg	wt	yes	yes	no	no	no	no	no	no	0	80	TP	FU	1,9	2,2	0,48		TP
69	f	60	GBM	IV	pos	mut	yes	yes	no	no	no	no	no	no	0	90	TRC	FU	1,9	1,5	0,21		TRC
70	f	43	A	II	n.d.	mut	yes	yes	no	no	no	yes	no	no	1	90	TP	FU	2,2	3,1	0,04		TP
71	m	60	GBM	IV	n.d.	wt	yes	yes	no	no	no	no	yes	no	1	100	TP	FU	2,0	2,1	-0,51		TP
72	m	36	A	III	pos	mut	yes	no	no	no	no	no	no	no	0	100	TP	FU	1,7	1,7	0,21	PET progressive	TP
73	f	66	ODG	II	n.d.	mut	no	yes	no	no	no	no	no	no	1	90	TP	FU	2,6	2,9	-0,71		TP
74	m	64	GBM	IV	pos	wt	yes	yes	yes	no	no	no	no	no	0	90	TP	FU	1,8	2,1	-0,41		TP
75	m	55	GBM	IV	n.d.	wt	yes	yes	no	no	no	no	no	no	0	100	TP	NP	1,8	2,1	0,42		TP
76	f	38	A	III	pos	mut	yes	yes	no	no	no	yes	no	no	2	90	TP	NP	1,3	1,3	0,15		TP
77	m	54	ODG	II	pos	mut	no	no	no	no	no	yes	no	no	1	100	TRC	FU	0,5	0,5	0,01		TRC
78	f	39	A	III	pos	mut	yes	yes	no	no	no	no	no	no	0	100	TP	FU	1,5	1,5	0,47		TRC
79	m	48	GBM	IV	neg	wt	yes	no	no	yes	no	yes	no	no	1	90	TP	FU	2,1	2,6	0,92		TP
80	f	58	A	III	neg	mut	yes	yes	yes	yes	no	no	yes	no	2	70	TP	FU	1,9	2,2	0,58		TP
81	f	45	GBM	IV	pos	mut	yes	no	no	yes	no	no	no	no	0	90	TP	NP	0,5	0,5	0,55		TRC
82	f	66	A	III	pos	wt	yes	yes	yes	no	no	no	no	no	1	90	TRC	FU	1,5	1,5	0,70		TRC
83	m	41	ODG	II	n.d.	mut	yes	yes	no	no	no	yes	no	no	2	100	TRC	FU	1,3	1,3	0,47		TRC
84	f	52	GBM	IV	n.d.	wt	yes	yes	yes	no	no	no	no	no	1	90	TRC	FU	1,4	1,4	1,66		TRC
85	m	53	A	II	n.d.	wt	yes	yes	no	no	no	no	no	no	0	80	TRC	FU	1,3	1,4	1,60		TRC
86	m	56	GBM	IV	neg	wt	yes	yes	no	no	yes	no	no	no	0	90	TP	FU	2,0	2,2	0,03		TP
87	m	45	A	III	pos	mut	yes	yes	no	no	no	no	no	no	0	100	TRC	NP	2,1	2,3	-0,60		TP
88	m	45	GBM	IV	neg	wt	yes	yes	no	no	no	no	no	no	0	100	TP	NP	2,1	2,2	0,54		TP
89	f	44	ODG	II	pos	mut	yes	no	no	no	no	no	no	no	0	100	TP	FU	1,4	1,4	0,71		TRC
90	f	42	GBM	IV	neg	wt	yes	yes	no	yes	no	no	no	no	0	70	TP	FU	2,1	2,9	-0,52		TP
91	m	53	A	III	neg	wt	yes	yes	no	no	no	yes	yes	no	1	100	TP	FU	2,0	2,1	0,25		TP
92	m	56	GBM	IV	n.d.	wt	yes	yes	no	no	yes	no	yes	no	1	90	TP	FU	2,0	2,4	-0,83		TP
93	f	58	GBM	IV	neg	wt	yes	no	no	no	no	no	no	no	0	90	TP	NP	1,6	1,6	0,49		TRC
94	m	50	GBM	IV	neg	wt	yes	yes	no	no	yes	no	no	no	0	70	TP	NP	1,8	2,0	0,68		TP
95	m	57	GBM	IV	neg	wt	yes	no	no	no	no	no	no	yes	0	90	TP	FU	2,0	2,1	-0,65		TP
96	m	75	GBM	IV	neg	wt	yes	no	no	no	no	no	no	yes	0	100	TP	NP	2,4	3,1	-0,28		TP

97	f	58	GBM	IV	neg	wt	yes	yes	no	no	no	no	no	no	0	100	TP	NP	2,3	2,7	0,16		TP
98	m	51	A	III	pos	mut	yes	yes	yes	no	no	yes	yes	no	3	100	TP	NP	1,4	1,4	0,16		TRC
99	f	58	other	n.d.	n.d.	n.d.	yes	yes	no	no	no	no	no	no	0	90	TRC	FU	1,3	1,3	1,22		TRC
100	f	33	A	III	neg	mut	yes	yes	no	no	no	no	no	no	0	100	TRC	FU	0,7	0,7	0,25		TRC
101	m	47	GBM	IV	pos	wt	yes	yes	no	no	no	no	no	no	0	100	TRC	FU	1,2	1,2	1,03		TRC
102	m	46	A	III	n.d.	mut	no	no	no	no	no	no	no	no	0	100	TP	FU	0,9	0,9	0,52		TRC
103	m	64	GBM	IV	neg	wt	yes	yes	no	no	no	no	no	no	0	90	TP	FU	2,1	2,7	-0,69		TP
104	m	67	GBM	IV	neg	wt	yes	yes	no	no	yes	no	no	no	0	70	TP	FU	2,4	2,6	-0,77		TP
105	m	46	A	III	n.d.	wt	yes	yes	no	no	yes	no	no	no	1	90	TP	FU	2,7	3,7	-0,67		TP
106	m	55	ODG	III	pos	mut	yes	no	yes	no	no	no	no	no	0	90	TRC	FU	2,0	2,3	0,44		TP
107	f	53	GBM	IV	pos	mut	yes	yes	no	yes	no	yes	yes	no	2	70	TP	FU	1,9	1,9	0,30	PET progressive	TP
108	m	52	GBM	IV	n.d.	wt	yes	yes	yes	no	no	no	no	yes	0	70	TP	FU	1,8	2,0	-0,78		TP
109	m	20	GBM	IV	pos	wt	yes	yes	yes	no	no	no	no	yes	0	100	TP	FU	1,4	1,4	0,79	Hot spot	TP
110	f	45	A	III	pos	mut	yes	yes	no	no	no	yes	no	no	2	90	TP	FU	2,1	2,7	1,82		TP
111	m	37	GBM	IV	pos	mut	yes	yes	no	no	no	no	no	yes	0	100	TP	FU	1,5	1,5	0,32		TRC
112	f	56	GBM	IV	neg	wt	yes	yes	no	no	no	no	no	no	0	100	TP	FU	1,8	1,8	-0,17		TP
113	m	63	GBM	IV	neg	wt	yes	yes	no	no	no	no	no	no	0	80	TP	FU	2,0	2,5	0,09		TP
114	f	34	A	III	n.d.	mut	yes	yes	no	no	no	no	no	no	0	100	TRC	NP	2,0	2,0	0,74		TP
115	f	39	ODG	III	pos	mut	yes	yes	yes	no	no	no	no	no	1	100	TRC	NP	1,9	2,2	0,02		TP
116	f	45	ODG	III	pos	mut	yes	yes	no	no	no	no	no	no	1	90	TP	NP	1,8	2,1	0,85		TP
117	m	39	A	II	n.d.	mut	yes	yes	no	no	no	no	no	no	0	100	TP	NP	1,4	1,4	0,68		TRC
118	m	34	A	II	n.d.	wt	yes	no	no	no	no	no	yes	no	1	90	TRC	FU	1,9	1,9	0,95		TRC
119	m	56	GBM	IV	neg	wt	yes	yes	no	no	no	yes	no	yes	1	100	TP	NP	1,9	2,0	-0,82		TP
120	m	45	GBM	IV	pos	wt	yes	yes	yes	no	no	no	no	no	1	90	TP	FU	2,4	3,5	-0,74		TP
121	m	41	GBM	IV	pos	mut	yes	yes	no	no	no	yes	yes	no	2	100	TP	NP	1,9	1,9	-0,39		TP
122	m	30	ODG	II	pos	mut	no	no	no	no	no	no	no	no	0	100	TRC	FU	1,1	1,1	0,20		TRC
123	m	69	GBM	IV	neg	wt	yes	yes	no	no	no	yes	yes	no	2	90	TP	NP	1,9	2,2	-0,59		TP
124	m	58	GBM	IV	pos	wt	yes	yes	no	no	no	no	no	no	0	100	TRC	FU	1,9	2,1	-0,14		TP
125	f	62	GBM	IV	pos	wt	yes	yes	no	no	yes	no	no	no	0	80	TP	FU	2,1	2,6	1,74		TP
126	m	53	GBM	IV	neg	wt	yes	yes	no	no	no	no	no	no	0	100	TP	NP	2,1	2,5	1,20		TP
127	m	46	A	III	neg	mut	yes	yes	yes	yes	no	yes	yes	no	1	100	TP	NP	2,0	2,2	0,59		TP

Legends:
m = male; **f** = female; **GBM =** glioblastoma; **A** = astrocytoma; **ODG** = oligodendroglioma 1p/19q codeleted; **DMG** = diffuse midline glioma, H3 K27M-mutant; **NOS** = not otherwise specified; **IDH** = isocitrate dehydrogenase ; **mut** = mutant; **wt** = wildtype; **n.d.** = not determined or inconclusive; **TP** = tumor progression; **TRC** = treatment-related changes; **NP** = neuropathology; **FU** = clinico-radiological follow-up; **TBR_{mean}** = mean tumor/brain ratio; **TBR_{max}** = maximum tumor/brain ratio; **Slope** = slope of the late phase of the time-activity curve of ^{18}F-FET-uptake in the tumor; **^{18}F-FET-PET rating**: TP if TBR_{max} > 1.95 or slope < 0.2 or special findings; **Hot spot** = focally increased ^{18}F-FET uptake in the tumor area that was underestimated in the ROI analysis and therefore rated as positive; **PET progressive** = increasing ^{18}F-FET uptake compared with a previous PET investigation leading to positive rating although the threshold values of ROC analysis were not exceeded

SUPPLEMENTAL TABLE 2

Diagnoses derived from ^{18}F-FET PET parameters and congruence of ratings from ^{18}F-FET PET and histology/follow-up

Diagnosis based on ^{18}F-FET PET findings	number	%
tumor progression	92	72
treatment-related changes	35	28
Diagnosis based on histology/follow-up		
tumor progression	94	74
treatment-related changes	33	26
Validation of diagnosis		
histology	40	31
follow-up	87	69
Consistency of diagnoses from ^{18}F-FET PET and histology/follow-up		
correct	103	81
incorrect	24	19

SUPPLEMENTAL TABLE 3

Findings from ^{18}F-FET PET versus diagnosis in all patients, based on histology and on follow-up, respectively

Assessment following ^{18}F-FET PET Diagnosis (histology, follow-up)	**Tumor progression**	**Treatment-related changes**	**Total**
Tumor progression	81	13	94
Treatment-related changes	11	22	33
Total	92	35	127
Assessment following ^{18}F-FET PET Diagnosis based on histology	**Tumor progression**	**Treatment-related changes**	**Total**
Tumor progression	29	5	34
Treatment-related changes	5	1	6
Total	34	6	40
Assessment following ^{18}F-FET PET Diagnosis based on follow-up	**Tumor progression**	**Treatment-related changes**	**Total**
Tumor progression	52	8	60
Treatment-related changes	6	21	27
Total	58	29	87